

Generation of Automated Label-Free Cell Migration Assays through the Incorporation of Magnetic 3D Bioprinting

Brad Larson¹, Leonie Rieger¹ and Glauco R. Souza^{2,3}

¹BioTek Instruments, Inc. | Winooski, VT | USA • ²Nano3D Biosciences, Inc. | Houston, TX | USA

³The University of Texas Health Science Center at Houston | Houston, TX | USA



Introduction

Cell migration involves a cyclical coordinated procedure starting with cell polarization, protrusion and substrate attachment of the leading edge, in addition to proteolytic degradation of physical barriers (e.g. tissue components and actinomyosin contraction) before the cell moves. Migration plays a central role in multiple beneficial physiological processes such as wound healing, in addition to being the first step in tumor metastasis as cells move away from the primary tumor site. Therefore, an advanced knowledge and methodology for monitoring phenotypic cell migration is useful for screening potential negative cytotoxic effects in test molecules, as well as speeding the development of novel therapies to re-establish wound healing abilities in pathologic tissue or control metastatic cellular invasion. Multiple techniques currently exist to assess cell migration. These commonly involve monitoring the migration of cells adhered to labware. The easiest and most sensitive of these methods incorporate label-free imaging to precisely track cell movement without introducing fluorescent probes that have the capability of changing normal cell activity. However, there are limitations to these migration assays. First, these assays use monolayers, which poorly mimic native tissue environments. In particular, these monolayers do not simulate tissue structure and properties, have altered cell exposure to compounds, and lack normal cell-cell and cell-extracellular matrix (ECM) interactions that characterize living tissue. Thus, cell migration witnessed in monolayers may misrepresent behavior seen *in vivo*.

Three-dimensional (3D) cell culture platforms are potential solutions as they can reconstruct tissue structure and environments *in vitro*. In particular, incorporation of magnetic 3D bioprinting, where cells are magnetized and printed into appropriate 3D cell cultures, provides a method to reestablish missing interactions and easily create 3D phenotypic cell migration assays. Using this method, cells are magnetized with a biocompatible nanoparticle assembly consisting of gold, iron oxide, and poly-L-lysine that electrostatically and non-specifically attaches to cell membranes. Magnetized cells can then be directed using mild magnetic forces to form aggregates where cells interact and build larger 3D environments with ECM that represent native tissues. Cells and matrix can then be printed into different configurations to assess wound healing and metastatic cell movement. Here we present two bioprinting procedures that were created to allow 3D wound healing and metastatic cell movement to take place *in vitro*. Label-free cell migration was tracked over time using automated widefield microscopy. Final combined processes were tested using multiple skin and cancer cell models in 384-well format to demonstrate that the incorporation of 3D magnetic bioprinting can lead to the generation of *in vivo*-like cell migration data.

BioTek Instrumentation

Cytation™ 5 Cell Imaging Multi-Mode Reader: Cytation 5 is a modular multi-mode microplate reader combined with automated digital microscopy. Filter- and monochromator-based microplate reading are available, and the microscopy module provides up to 60x magnification in fluorescence, brightfield, color brightfield and phase contrast. The instrument can perform fluorescence imaging in up to four channels in a single step. With special emphasis on live-cell assays, Cytation 5 features shaking, temperature control to 65 °C, CO₂/O₂ gas control and dual injectors for kinetic assays, and is controlled by integrated Gen5™ Microplate Reader and Imager Software, which also automates image capture, analysis and processing. The instrument was used to kinetically monitor wound closure and cell migration activity using the brightfield channel.

Magnetic 3D Bioprinting and Levitation

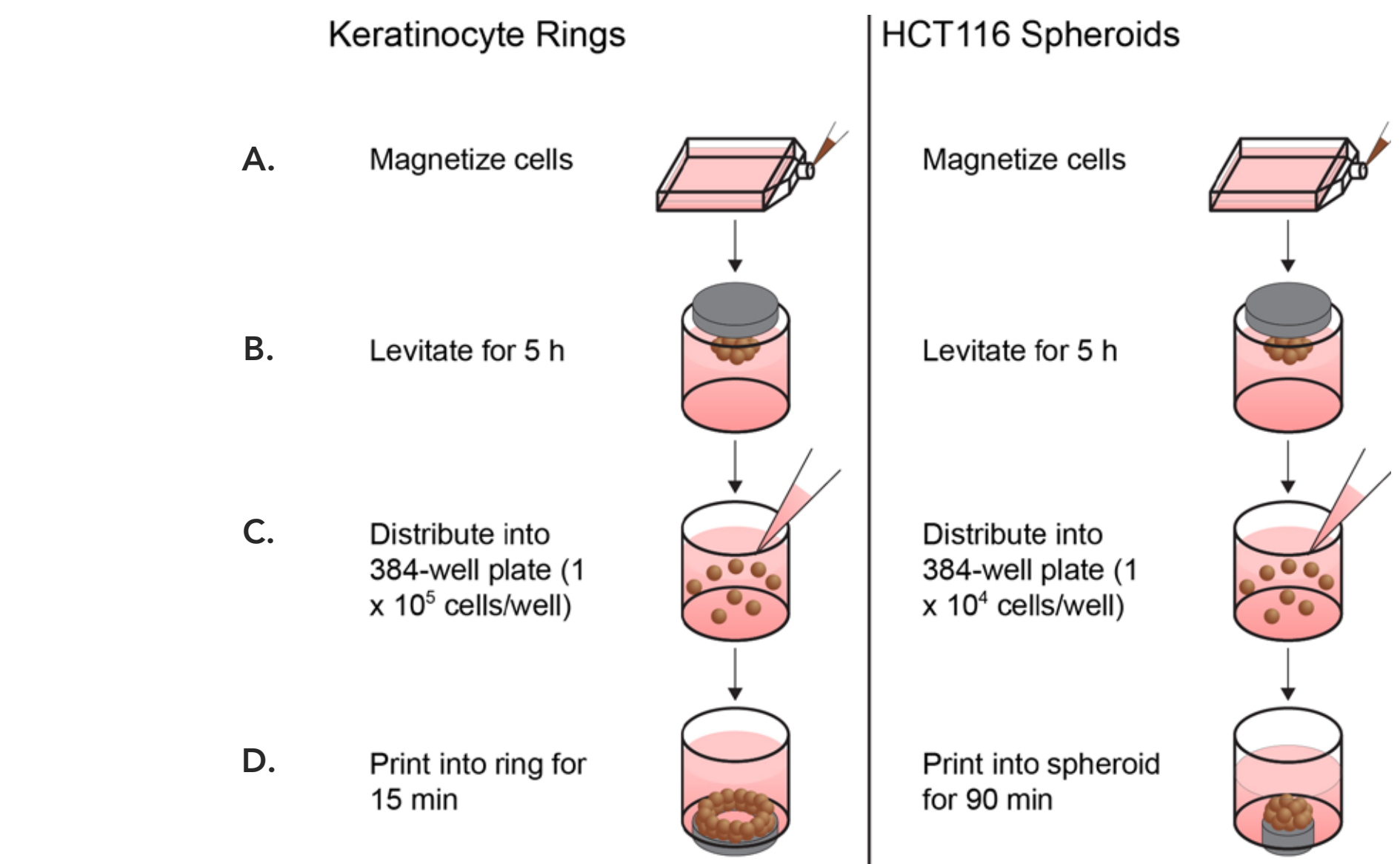


Figure 1. Bio assay kit protocol. The 384-Well Bio Assay™ Kit uses NanoShuttle™-PL, a nanoparticle assembly consisting of gold, iron oxide and poly-L-lysine to (A) magnetize cells. After incubation, (B) cells are detached, resuspended in a cell-repellent plate, and magnetically levitated to aggregate and induce ECM. After breaking up the aggregates, (C) single cells are transferred to a 384-well cell-repellent plate, and (D) placed atop a 384-well magnet, where they aggregate at the well bottom in the shape of the magnet (ring configuration shown at left; spheroid configuration shown at right).

Materials and Methods

Cells, Assay and Experimental Components: Immortalized keratinocytes (Catalog No. CRL-2309) and HCT116 colorectal carcinoma cells (Catalog No. CCL-247) were purchased from ATCC (Manassas, VA). The 384-Well Bio Assay Kit (GBO Catalog No. 781846, consisting of 2 vials NanoShuttle-PL, 6-Well Levitating Magnet Drive, 384-Well Spheroid and Holding Magnet Drives (2), 96-Well Deep Well Mixing Plate, 6-Well and 384-Well Clear Cell Repellent Surface Microplates), prototype 384 well Ring Drive, and additional Cell Repellent Surface 6-Well (GBO Catalog No. 657860) and 384-Well Black µClear® Microplates (GBO Catalog No. 781976), were generously donated by Nano3D Biosciences, Inc., and Greiner Bio-One, Inc., (Monroe, NC). Ordonin (Catalog No. O9639) was purchased from Sigma-Aldrich (St. Louis, MO). Rapamycin (Catalog No. BML-A275) and KU-0063794 (Catalog No. ENZ-CHM135) were generously donated by Enzo Life Sciences (Farmingdale, NY).

Assay Procedure: Cells were prepared for magnetic bioprinting and levitation, including treatment with NanoShuttle-PL, according to the manufacturer's protocol. After preparation, cells were added to the 6-well cell repellent plate, and a 6-well magnet was placed atop each well plate to levitate the cells, where they aggregated into 3D structures and induced ECM formation during a five hour incubation at 37 °C/5% CO₂. After incubation, the cells and ECM were broken up, resuspended and added to 384-well cell repellent plate wells.

For wound healing tests, the total concentration of keratinocytes added to the 384-well cell repellent plate wells was 1.0x10⁵ cells/well in a volume of 40 µL. A 384-well ring magnet was placed below the well plate, and the assembly was incubated at 37 °C/5% CO₂ for 15 minutes to allow cells to aggregate into the magnet's ring shape. Then, 10 µL of 5x titrations of 200, 100 or 0 µM oridonin was added to the wells, and the plate was placed into Cytation 5, preset to 37 °C/5% CO₂ where kinetic brightfield imaging, using a 4x objective, was performed every 30 minutes for 16 hours.

For cell migration tests, the total concentration of HCT116 cells was 1.0x10⁴ cells/well in a volume of 40 µL. A 384-well spheroid magnet was placed below the well plate, and the assembly was incubated at 37 °C/5% CO₂ for 90 minutes to allow cells to aggregate into a spheroid. Then, 10 µL of 5x titrations of 200, 100, or 0 µM rapamycin or KU-0063794 was added to the wells, and the plate was placed into Cytation 5, preset to 37 °C/5% CO₂ where kinetic brightfield imaging, using a 2.5x objective, was performed every 15 minutes for 48 hours.

Label-Free Image-Based 3D Wound Healing Monitoring

The ability of the 3D bioprinted ring structure to demonstrate wound healing, and the capability of automated image-based monitoring and analysis was initially examined. As seen in Figures 2A and 2B, the untreated keratinocyte 3D ring structure contracted over time, while oridonin had an inhibitory effect on wound closure (Figures 2C and 2D). This also demonstrated Cytation 5's ability to track 3D cellular movement throughout the entire incubation period.

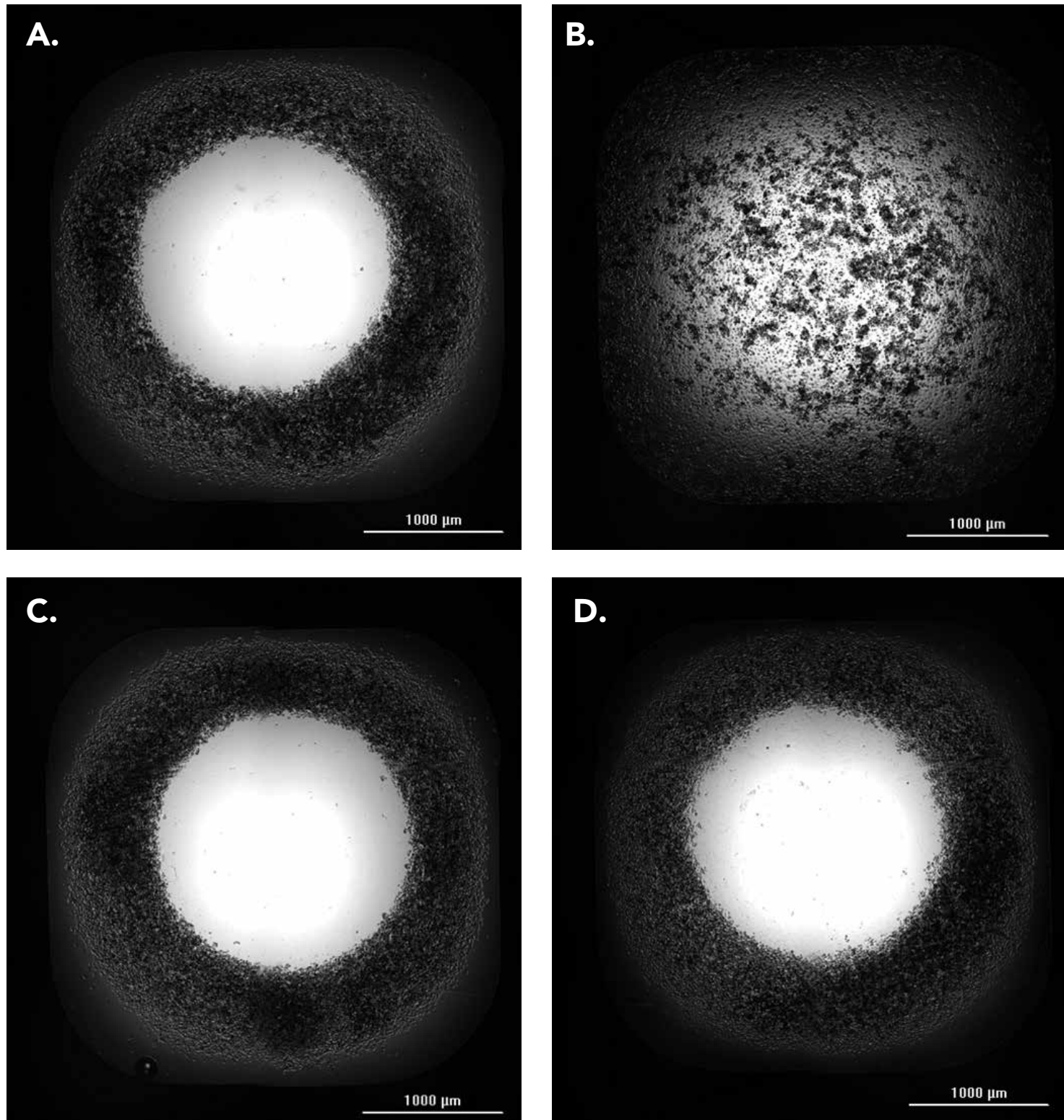


Figure 2. Wound healing using 3D bioprinted keratinocyte ring structures. Stitched brightfield images of 3 row by 2 column montage tiles, using a 4x objective, treated as follows: (A) 0 µM oridonin, 0 hours incubation; (B) 0 µM oridonin, 16 hours incubation; (C) 40 µM oridonin, 0 hours incubation; (D) 40 µM oridonin, 16 hours incubation.

Original brightfield images were then pre-processed (Figure 3A) to smooth the background signal and remove the halo effect seen in brightfield imaging (Figure 3B). An image plug was then placed on each image of appropriate size to always include a portion of the ring structure. Upon placement, cellular analysis was conducted using parameters such that the contrast between signal from the bioprinted ring area and background (Figure 3C) was used to place accurate object masks around the portion of the cellular area within each mask (Figure 3D). Use of pre-processed images improved the accuracy of object mask placement. Through use of this analysis procedure, the total cell and ECM area within the plug at time 0, and throughout the incubation period could be tracked.

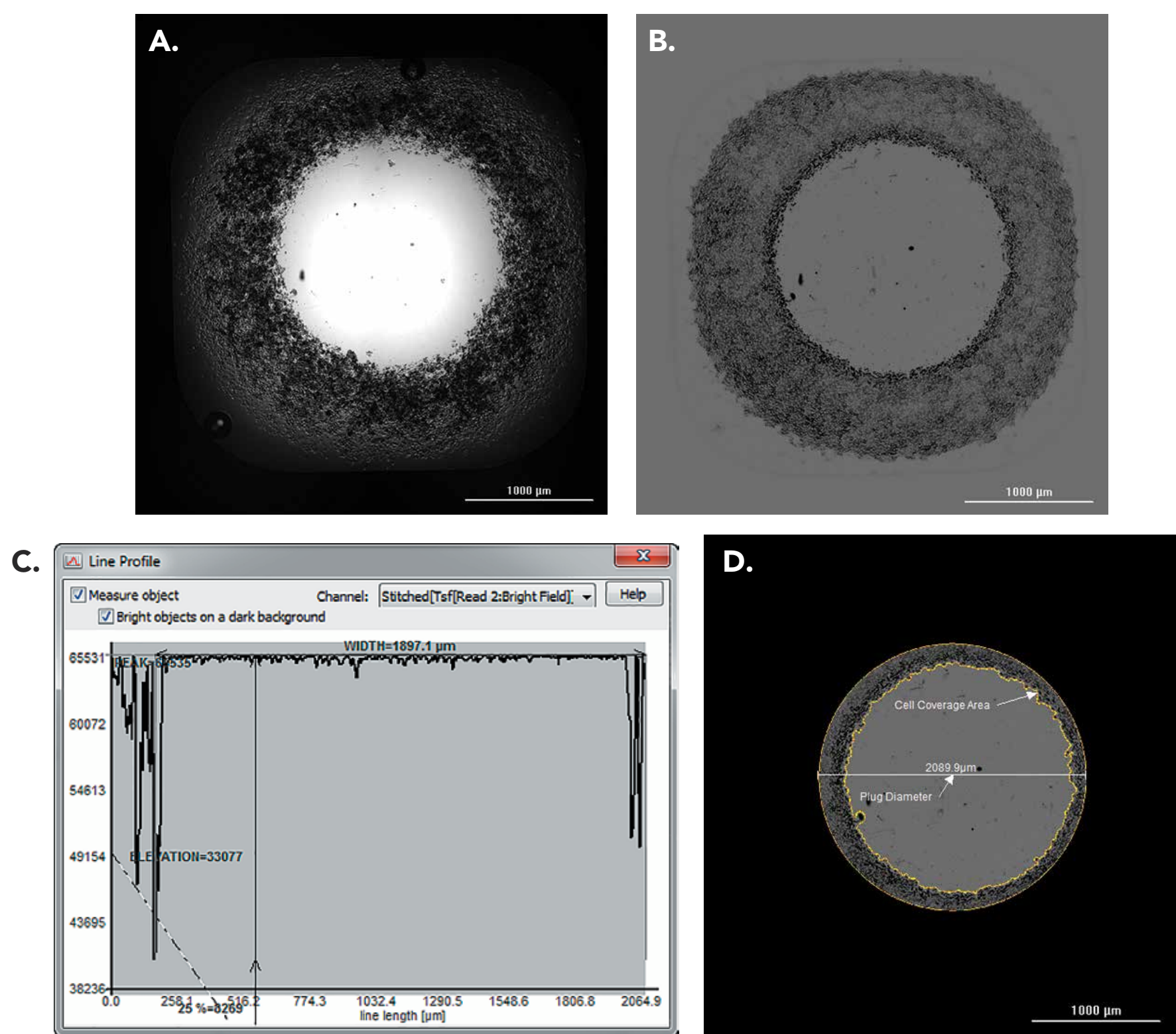


Figure 3. Gen5 cellular analysis of 3D wound healing images. Representative (A) unprocessed, and (B) pre-processed brightfield image, captured using a 4x objective and 3x2 image montage. (C) Graph of brightfield signal across the diameter of the image plug through areas containing cells and non-cellular areas. (D) Representative cellular analysis image showing plug diameter and object mask placement around the cellular area within the plug.

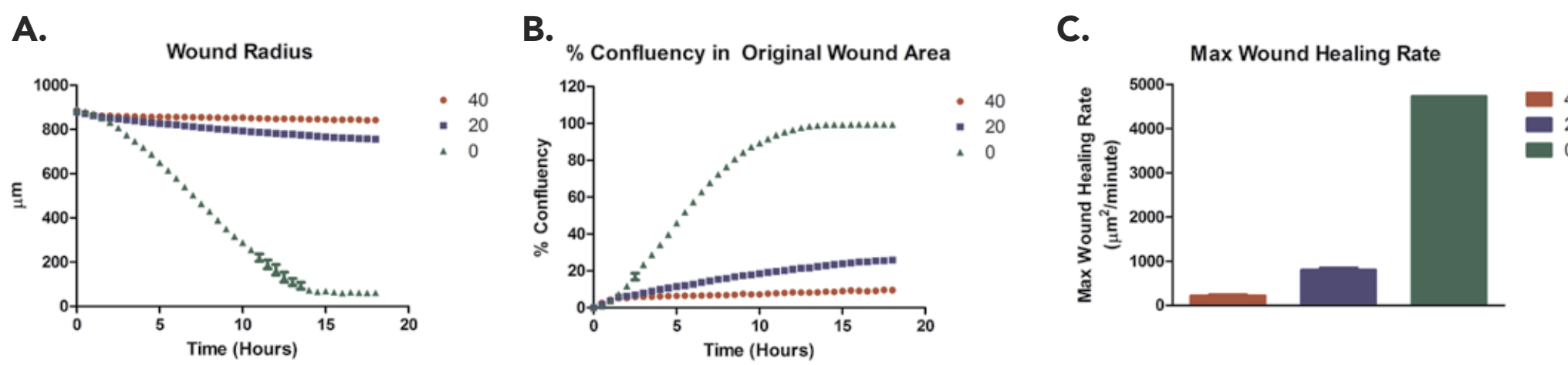


Figure 4. Calculated kinetic 3D wound healing graphs. Graphs of (A) wound radius, (B) % cell confluency in the original wound, and (C) maximum wound healing rate plotted for vehicle, 20 and 40 µM oridonin.

The Gen5 calculated metric of Sum Area_i (total cellular area within the plug) was used to quantify multiple metrics of cell migration as a function of time in the kinetic assay. Wound radius was the radius of the circular area uncovered by cells within each image plug. Percent confluency in the original wound area was the area of cells and ECM migrating into the original calculated wound area, expressed as a percentage, and maximum wound healing rate was the highest rate of slope increase, or V_{max}, from the kinetic % confluency in the original wound graphs. Each metric was also automatically calculated by Gen5 and used to determine the uninhibited healing rate of test cell types, or the ability of molecules to modify initial rates of wound healing.

For experiments conducted here, the keratinocyte/ECM combination migrated at a rate where complete wound closure was seen within 14 hours. Migration was then modified by oridonin, such that near complete inhibition could be achieved using a 40 µM concentration. These findings confirm the ability of the 3D image-based assay procedure for use with wound healing applications.

Label-Free 3D Cell Migration Monitoring

Detection and quantification of metastatic cell migration was then examined using a similar 3D bioprinting and image-based analysis procedure. Brightfield images were captured of HCT116 cells and ECM migrating away from the original bioprinted area over the incubation period (Figure 5A). Image pre-processing was again performed to remove the dark areas of the image, allowing easier visualization of the leading edges of the migrating structure which have a minimal change in contrast with the image background (Figure 5B). HCT116 cell migration could then be visualized (Figures 5C and 5D), as well as interruption of cell movement by 10 µM concentrations of the known inhibitors rapamycin (Figures 5E and 5F) and KU-0063794 (Figures 5G and 5H).

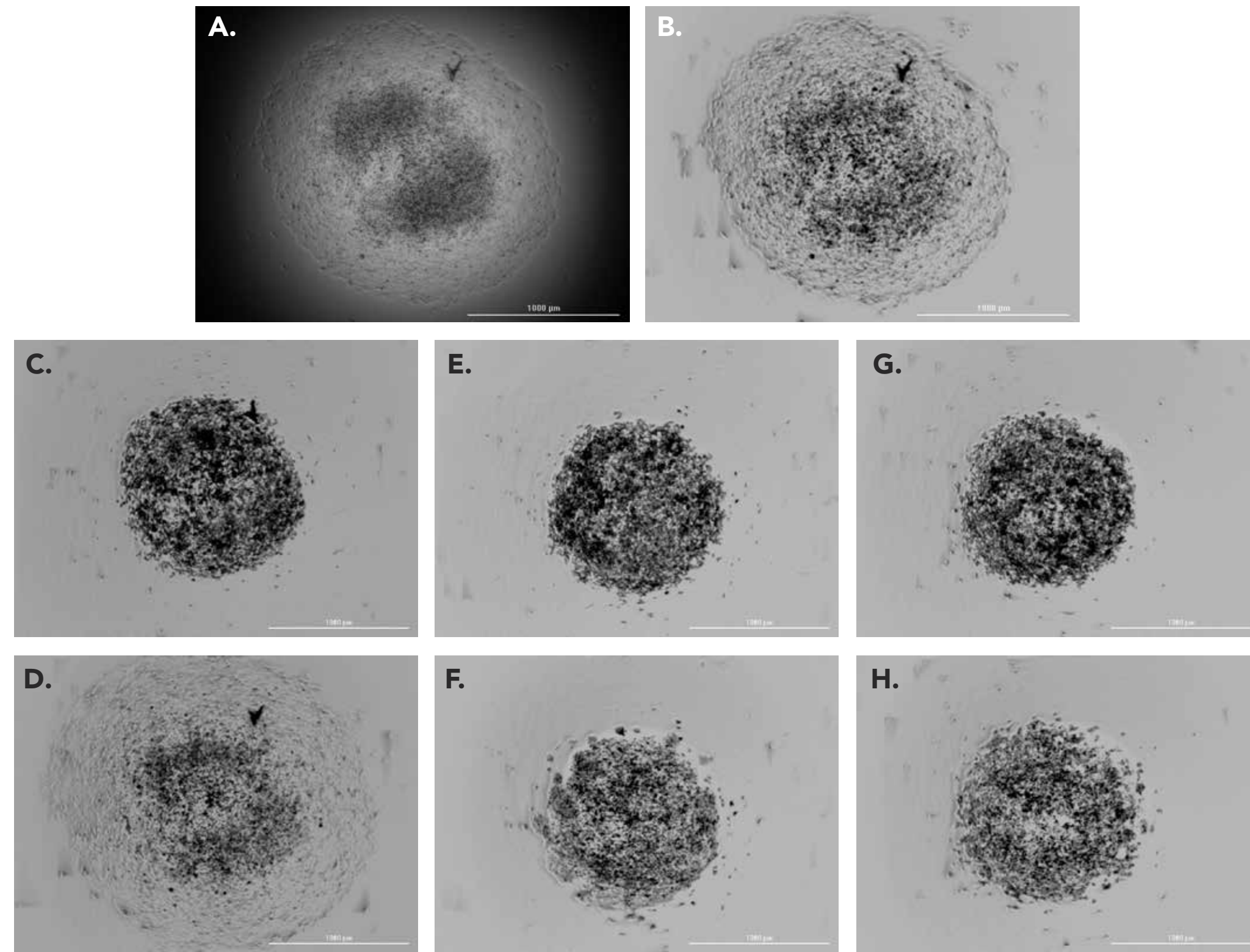


Figure 5. Cell and ECM migration in 3D bioprinted HCT116 cells and ECM. (A) Unprocessed and (B) pre-processed brightfield images captured using a 2.5x objective. Pre-processed images of 3D printed cells treated as follows: (C) untreated, 0 hours incubation; (D) untreated, 48 hours incubation; (E) 10 µM rapamycin, 0 hours incubation; (F) 10 µM rapamycin, 48 hours incubation; (G) 10 µM KU-0063794, 0 hours incubation; (H) 10 µM KU-0063794, 48 hours incubation.

Using Gen5 software, object masks were placed around the migrating structure; once again using the changes in brightfield signal between areas of the image containing cells and ECM and non-cellular background areas (Figure 6A). The process allowed detailed object mask placement (Figure 6B), and accurate tracking of cell movement.

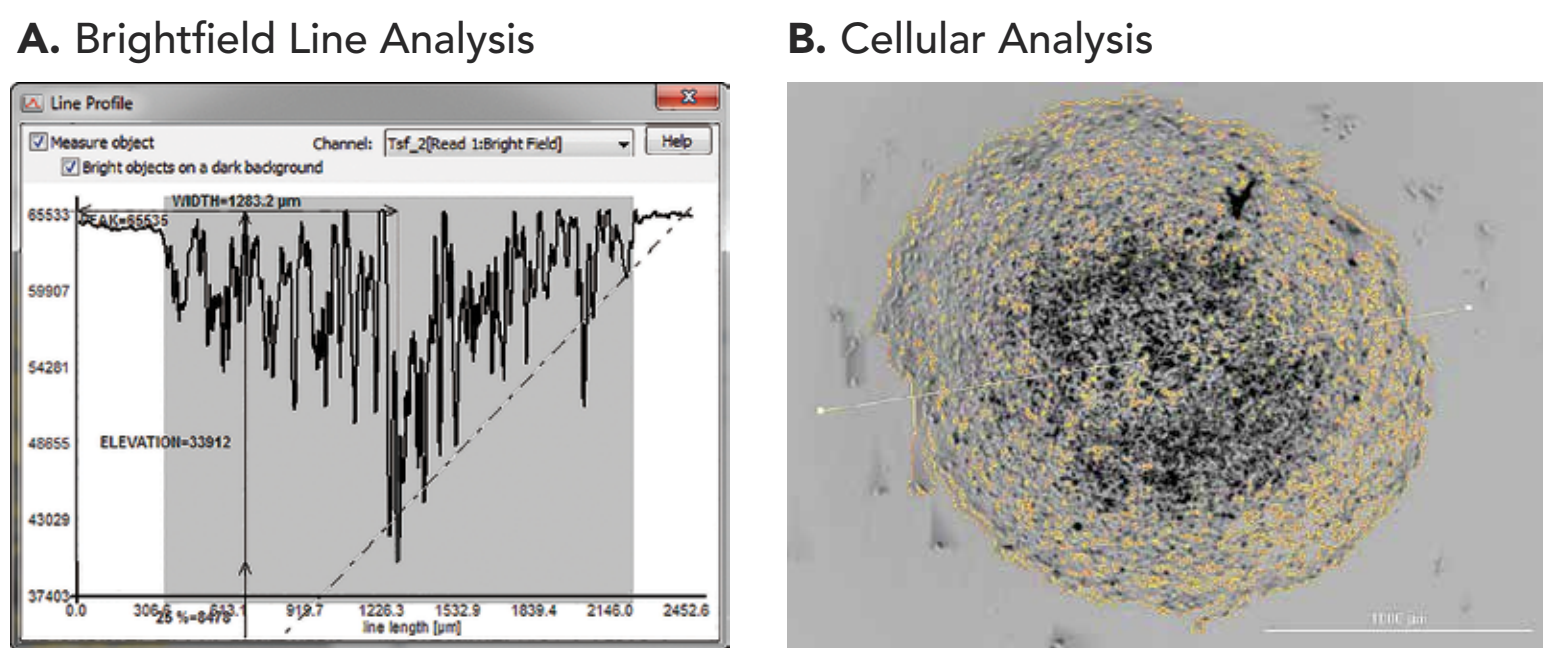


Figure 6. Image background signal removal via pre-processing. Representative brightfield image, using a 2.5x objective. (A) Line analysis showing change in brightness intensity from the middle of the 3D spheroid to the edge; (B) object masks automatically placed around cells using Gen5 Software.

Area within each object mask was automatically returned by Gen5 as a calculated metric at each time point for the rapamycin and KU-0063794 concentrations tested. Coverage area values, along with fold change values calculated by comparing object areas at each timepoint to those from time 0, were then graphed.

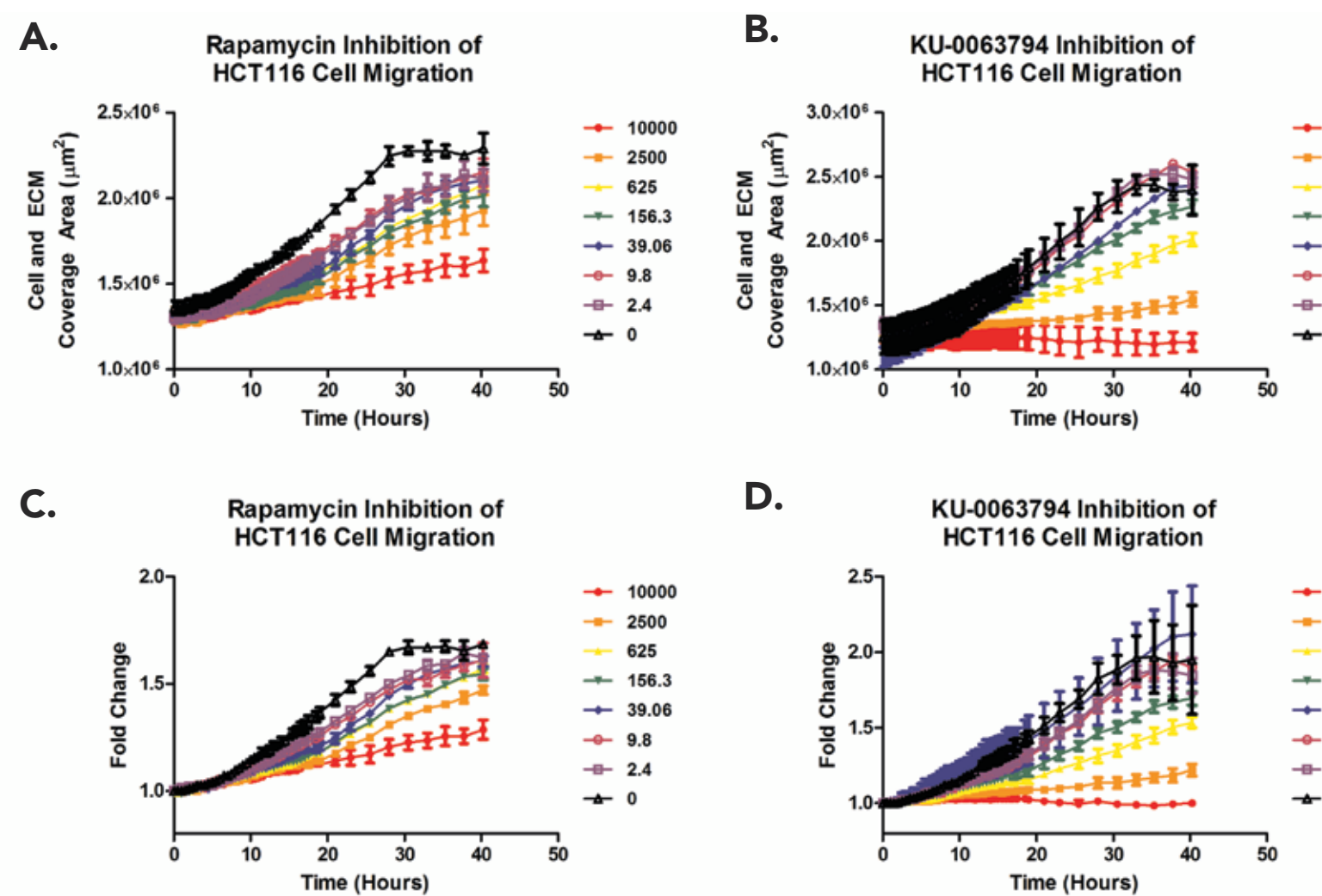


Figure 7. Kinetic HCT116 cell migration analysis. Coverage area of cells exposed to 0-10,000 nM (A) rapamycin; or (B) KU-0063794. (C) Rapamycin; and (D) KU-0063794 area fold change calculations compared to coverage area at time 0.

The results in Figure 7 demonstrate that both rapamycin and KU-0063794 have a dose dependent effect on HCT116 cell and ECM movement, and further validates the use of the 3D bioprinting and image-based process to assess metastatic cell migration.

Conclusions

- The 384-Well Bio Assay Kit and NanoShuttle-PL particles from n3D Biosciences provide a simple, high-throughput method to carry out biomimetic, 3D determinations of wound healing and metastatic cell migration.
- The automated imaging capabilities of Cytation 5 simplify the experimental process by allowing label-free tracking of cell/ECM movement.
- Advanced cellular analysis tools in Gen5 software allow accurate and detailed analysis, with all data generated by a single instrument.
- The combination of assay method and automated imaging and analysis create a robust, high-throughput method to generate *in vivo*-like assessments of 3D cell movement.